Fourier-Transform Infrared Spectroscopy Analysis of the Changes in Chemical Composition of Wooden Components in the Ancient Building of Xichuan Guild Hall

Yan Yang He Sun Bin Li Aifeng Wang Rui Zhao
Wei Wang Yiming He Shuang Yang Yanxia Han
Wenye Sun

Abstract

In order to investigate the decay mechanism in red oak (*Quercus rubra*) and Schima (*Schima* spp.) wood in the ancient building of Xichuan Guild Hall, the changes in chemical composition were determined using Fourier-Transform Infrared Spectroscopy. The results were as follows: (1) The absorption peak intensities that represented the structural contribution of carbohydrates, and the crystallinity index of the cellulose in the red oak components, decreased noticeably by 55.70 percent in H1039/H1508, and 26.85 percent in H1370/H2900; while those of lignin were increased as a result of the brown rot process. These changes indicated that the brown-rot fungi had stronger degradation effects on hemicellulose and cellulose over lignin. (2) The absorption peak intensities of the carbohydrates (a part of the lignin) and the crystallinity index of the cellulose decreased noticeably by 22.50 percent in H1039/H1508, 25.00 percent in H1508/H1735, and 21.74 percent in H1429/H897 after white rot in the Schima wood components. These findings indicated that not only cellulose and hemicellulose but also lignin were attacked by white-rot fungi. By comparison, the extent of fungal damage in the wood components was lower in the Schima wood components than that in the red oak components.

The Xichuan Guild Hall, which was built in about 1910, is located at No. 261, Democracy St., Wancheng District, Nanyang City, Henan Province, China, and is considered a key cultural relic protection unit of Nanyang City. However, its wooden components have shown signs of degradation as a result of exposure over the years, including changes in their anatomical structure, chemical composition, and reduction in physical and mechanical properties (Ferraz and Durán 1995, Choi et al. 2006, Arias et al. 2010, Koyani et al. 2014, Bari et al. 2019, Brischke et al. 2019, Chang et al. 2019, Gao et al. 2019, Li et al. 2019). These reductions eventually affect the quality and life span of the Hall.

Fourier-Transform Infrared Spectroscopy (FTIR; Stark and Matuana 2004, 2007; Huang et al. 2012; Tamburini et al. 2017; Croitoru et al. 2018; Fahey et al. 2019; Wentzel et al. 2019) is an effective technique for investigating the chemistry of wood, especially decayed wood components in ancient buildings. FTIR has certain advantages when used in conjunction with ancient buildings, including: (1) it requires a minimal number of samples and sample preparation compared with conventional gravimetric techniques (Pandey and Pitman 2003, Xu et al. 2013); and (2) it results in

The authors are, respectively, Associate Professor, School of Architecture, Nanyang Inst. of Technol., China (yangyanrainy@163.com [corresponding author]); Doctoral Candidate, College of Materials Sci. and Engineering, Southwest Forestry Univ., Kunming City, China (1066659587@qq.com); Associate Professor, Lecturer, Lecturer, Lecturer, and Lecturer, School of Architecture, Nanyang Inst. of Technol., China (165400683@qq.com, 13461945630@163.com, 515928346@qq.com, 659774129@qq.com, 1024774557@qq.com); Undergraduate, School of Economics, Henan Univ. Minsheng College, Kaifeng City, China (2729153423@qq.com); and Undergraduate and Undergraduate, School of Architecture, Nanyang Inst. of Technol., China (1723586353@qq.com, 1932741108@qq.com).
This paper was received for publication in May 2020. Article no. 20-00028.

Forest Prod. J. 70(4):448–452.
doi:10.13073/FPJ-D-20-00028

less damage to the building. Analyzing the changes in chemical composition can provide reference and guidance regarding degradation mechanisms, maintenance, and reinforcement of decayed wooden components.

The goal of this study was to better understand the changes in chemical composition and investigate the degradation mechanism of wood components in the ancient building of Xichuan Guild Hall. FTIR was used for chemical analyses to provide insights into the degradation process of wooden components exposed to fungi, weathering from ultraviolet light, etc., over time.

Materials and Methods

Materials

Samples were collected from the decayed wooden components in the ancient building of Xichuan Guild Hall in Nanyang City, Henan Province, China (Table 1; Sun et al. 2020, Yang et al. 2020b). Among the wooden component samples, sample No. 3 was obtained from the top surface of a red oak (*Quercus* sp.; Fagacae) beam and No. 1 was obtained from the side surface of an indoor Schima (*Schima* sp.) column (Yang et al. 2020b). Undecayed samples of *Quercus* sp. and *Schima* sp. were obtained from the Southwest Forestry University. The wood powder needed for FTIR analysis was processed using a grinder (XL-108, Guangzhou Xulang Machinery Equipment Co., Ltd, China) equipped with a 100-mesh screen (Yang et al. 2020a).

Method of FTIR analysis

For FTIR analysis, oven-dried wood powder and spectrum potassium bromide (KBr) were fully mixed in a ratio of 1:150, poured into an agate mortar, and ground into powdered form while keeping the wood powder and KBr in dried condition by using a high-wattage lamp throughout the whole process. The powder mixture was compressed into sliced samples using a powder tablet press machine (FW-4A, Uncommon Technology Development Co., China). To ensure the accuracy of the FTIR spectra, the sliced samples cannot have chipped edges and must have a uniform thickness. FTIR spectra were generated using an FTIR spectrophotometer (ALPHA2, Bruker Inc., Germany) in the range of 4,000 to 400 cm^{-1} to provide detailed information on the functional groups present in the sample surface (Yang et al. 2015, 2020a). Scans were run at a resolution of 4 cm^{-1}, and the spectra were obtained using attenuated total reflectance. In order to avoid the effect of experimental error, a minimum of five scans per specimen were operated to calculate their average.

Lignin peaks were compared with hemicellulose and cellulose peaks to evaluate relative changes in the composition of wooden components (Pandey and Pitman 2003, Xu et al. 2013).

The ratio of peak heights at 1,374 and 2,900 cm^{-1} (H1374/H2900) and 1,429 and 897 cm^{-1} (H1429/H897) was used to determine the cellulose crystallinity index in wood (Monrroy et al. 2011, Tomak et al. 2013).

Results and Discussion

FTIR analysis of red oak wooden components

Figure 1 shows the absorption peak intensity of the C=O stretching vibration of unconjugated carbonyl groups, acetyl, or carboxylic acid at 1,735 cm^{-1}, which is attributed to hemicellulose (xylans [Pandey and Pitman 2003, Ibrahim et al. 2007, Pandey and Nagveni 2007, Li et al. 2010, Monrroy et al. 2011, Zeng et al. 2012, Tomak et al. 2013, Xu et al. 2013, Liu et al. 2017]), as shown in Table 2. The fungal-decayed wood components were weakly degraded, which indicated a decrease in the small quantity of C=O (i.e., a subsequent reduction of hemicellulose contents). The absorption peak intensity at 810 cm^{-1} assigned to the mannose structure of hemicellulose was slightly decreased, indicating that a small part of the mannose structure was also degraded by the fungus (Fig. 1).

The characteristic peaks of 1,374, 1,336, 1,159, 1,039, and 897 cm^{-1} represent the structural contribution of carbohydrates (Pandey and Pitman 2003, Ibrahim et al. 2007, Pandey and Nagveni 2007, Li et al. 2010, Monrroy et al. 2011, Zeng et al. 2012, Tomak et al. 2013, Xu et al. 2013, Liu et al. 2017; Table 2). However, the absorption peak at 1,039 cm^{-1} disappeared and was replaced by two small absorption peaks at 1,050 and 1,040 cm^{-1} (Fig. 1). This finding indicated that the carbohydrates were degraded by fungi, leading to a decrease in the cellulose and hemicellulose contents. Figure 1 shows that the absorption peak intensity at 897 cm^{-1} was also weakened, also indicating a reduction in cellulose content. The absorption peak intensities at 1,374, 1,336, and 1,159 cm^{-1} in the fungal-decayed wood components also changed relative to those in the nondecayed wood components, indicating that the cellulose was attacked by fungi.

These characteristic peaks of 1,650, 1,600, 1,508, 1,460, 1,424, 1,232, and 1,120 cm^{-1} are the structural contributions associated with lignin (Pandey and Pitman 2003, Ibrahim et al. 2007, Pandey and Nagveni 2007, Li et al. 2010, Monrroy et al. 2011, Zeng et al. 2012, Tomak et al. 2013, Xu et al. 2013, Liu et al. 2017; Table 2). Their intensities, especially at 1,650, 1,508, 1,460, 1,232, and 1,120 cm^{-1}, were noticeably higher than those in nondecayed wood components (Fig. 1). These values indicated a relative increase in lignin content for the decayed wood components. The elevated absorption peaks of lignin showed the increase in phenolic hydroxyl content. In general, characteristic lignin peaks increase with the progression of decay. A high absorption peak intensity indicates great increase in decay

Table 1.—Information about the materials used.

Samples			
No.	Full name	Abbreviation	Sample location
3	The decayed red oak wood	DROW	Wooden column
Control	The nondecayed red oak wood	NDROW	Model specimens of the Southwest Forestry University
1	The decayed Schima wood	DSW	Wooden beam
Control	The nondecayed Schima wood	NDSW	Model specimens of the Southwest Forestry University

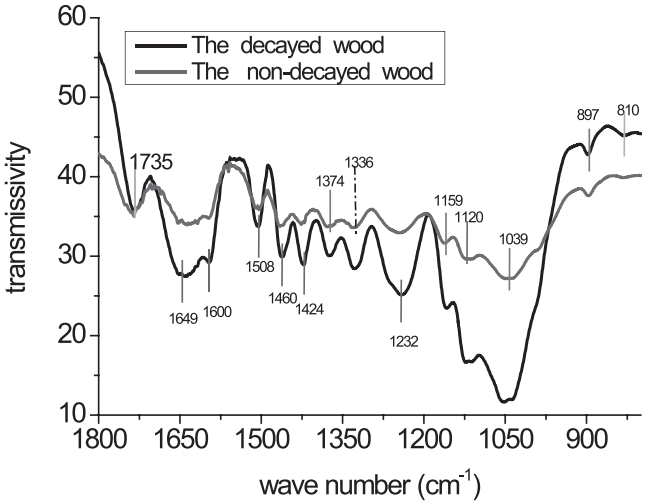

Figure 1.—Infrared spectrum of the red oak wood components: the region from 1,800 to 800 cm^{-1}.

degree (Pandey and Pitman 2003, Pandey and Nagveni 2007).

Brown-rot fungi only degrade carbohydrates and retain lignin, whereas white-rot fungi can consume not only cellulose and hemicellulose, but also lignin (Guo et al. 2010). Based on the analysis of the absorption peak intensities of cellulose, hemicellulose, and lignin, we concluded that cellulose and hemicellulose had decayed, whereas lignin was retained. Hence, we speculated that the red oak wooden components were attacked by brown-rot fungi. This finding is consistent with the microstructures of polarized light and fluorescence (Yang et al. 2020b).

In order to determine the difference of wood powder content and the influence of operation error on the experimental results, the ratios of the absorption peak intensities of lignin and carbohydrates were used to represent the changes in chemical composition (Li et al. 2010, Xu et al. 2013, Liu et al. 2017). The average relative intensities of lignin peaks at 1,649, 1,600, and 1,508 cm^{-1} against carbohydrate peaks at 1,735, 1,374, 1,159, and 1,039 cm^{-1} were calculated using the peak heights (Table 3). The changes in lignin content were characterized by the values of H1508/H1735, H1508/H1374, H1508/H1159, H1508/H1039, H1649/H1039, and H1600/H1039; whereas those for carbohydrate content were characterized by the values of H1735/H1508, H1374/H1508, H1159/H1508, and H1039/H1508 (Li et al. 2010, Xu et al. 2013, Liu et al. 2017). The carbohydrate contents were reduced (Table 3). These reductions in H1735/H1508, H1374/H1508, H1159/H1508, and H1039/H1508 ratios were 6.67, 6.32, 23.33, and 55.70 percent, respectively. Meanwhile, lignin contents increased (Table 3). The increase in H1508/H1735, H1508/H1374, H1508/H1159, H1508/H1039, H1649/H1039, and H1600/H1039 was 7.37, 6.67, 29.73, 126.40, 91.74, and 101.64 percent, respectively. These changes indicated that the fungi had a stronger preference to degrade hemicellulose and cellulose than lignin. These findings agree with those reported in previous studies (Li et al. 2010, Xu et al. 2013).

H1374/H2900 decreased from 1.08 in the nondecayed wood components to 0.79 in the fungal-decayed wood components, and H1429/H897 decreased from 0.92 to 0.70 (Table 3). These reductions were 26.85 and 23.91 percent for H1374/H2900 and H1429/H897, respectively. These results showed that both the amorphous and crystalline zones of cellulose were degraded (Monrroy et al. 2011). These reductions would decrease the crystallinity, which would also result in a reduction in physical and mechanical properties of wood. These findings were in good agreement with a previous study (Monrroy et al. 2011).

Table 2.—The Fourier-Transform Infrared Spectroscopy characteristic bands of the wood samples studied.

Wavenumber (cm^{-1})	Main band assignments and explanation
2,900	C–H stretching vibration
1,735	C=O stretching vibration of unconjugated carbonyl groups, acetyl or carboxylic acid (hemicelluloses)
1,649	C=O stretching vibration of conjugated carbonyl groups (lignin)
1,600	C–C stretching vibration of aromatic ring (lignin)
1,508	C–C stretching vibration of aromatic ring (lignin), stronger guaiacyl unit than syringyl unit
1,460	C–H deformation vibration (cellulose); asymmetric bending in CH_3 (lignin)
1,424	CH_2 scissor vibrations (cellulose); aromatic ring skeletal vibrations (lignin)
1,374	C–H deformation vibration (cellulose and hemicellulose)
1,336	OH in plane bending (cellulose)
1,260	C–O guaiacyl unit (lignin)
1,232	C–O stretching (hemicelluloses such as xylan); syringyl (lignin)
1,159	C–O–C stretching vibration (cellulose and hemicellulose)
1,120	guaiacyl and syringyl (lignin)
1,104	OH associated absorption band (cellulose)
1,039	C=O stretching vibration (cellulose and hemicellulose)
897	C–H deformation (cellulose)
810	mannose structure (hemicellulose)

FTIR analysis of Schima wooden components

Hemicellulose of Schima wood was heavily degraded as a result of fungal decay (Fig. 2). The absorption peak of 1,735 cm^{-1}, which is attributed to hemicellulose, had disappeared as a result of the degradation of glucurono-xylanes connected to the splitting of acetyl groups and 4-O-methylglucuronic acids side units (Solár et al. 2007). This finding indicated a marked reduction of the number of C=O linkages, resulting in a sharp decrease in hemicellulose content. No noticeable changes were found in the absorption peak intensity at 810 cm^{-1}, indicating that the mannose structure was not degraded by the fungi (Fig. 2).

Peaks at 1,374, 1,336, 1,159, 1,104, 1,039, and 897 cm^{-1} were attributed to the structural contributions of cellulose and hemicellulose. The absorption peaks of 1,159 and 1,104 cm^{-1} disappeared in the fungal-decayed wood components, indicating the degradation of celluloses and hemicelluloses with the resulting reductions in their content (Fig. 2). The absorption peak intensities at 1,374, 1,336, 1,039, and 897 cm^{-1} in the fungal-decayed wood components did not change noticeably compared with those in the nondecayed wooden components, indicating that the cellulose and hemicellulose contents at these absorption peaks did not markedly decrease (Fig. 2).

The characteristic peaks of 1,650, 1,600, 1,508, 1,460, 1,424, 1,260, 1,232, and 1,120 cm^{-1} are the structural contributions of lignin. The absorption peak of 1,650 cm^{-1}

Table 3.—The ratio of Fourier-Transform Infrared Spectroscopy characteristic peak height of wood samples studied. Note: +: increase percentage; −: decrease percentage.

	Average relative intensities of carbohydrate peaks against lignin peaks				Average relative intensities of lignin peaks against carbohydrate peaks						Cellulose crystallinity	
Samples[a]	H1735/ H1508	H1374/ H1508	H1159/ H1508	H1039/ H1508	H1508/ H1735	H1508/ H1374	H1508/ H1159	H1508/ H1039	H1649/ H1039	H1600/ H1039	H1370/ H2900	H1429/ H897
NDROW	1.05	0.95	0.90	0.79	0.95	1.05	1.11	1.25	1.21	1.22	1.08	0.92
DROW	0.98	0.89	0.69	0.35	1.02	1.12	1.44	2.83	2.32	2.46	0.79	0.70
Changes (%)	−6.67	−6.32	−23.33	−55.70	+7.37	+6.67	+29.73	+126.40	+91.74	+101.64	−26.85	−23.91
NDSW	0.96	0.96	0.91	0.80	1.04	1.04	1.10	1.25	1.23	1.23	1.02	0.92
DSW	1.28	1.00	0.88	0.62	0.78	1.00	1.14	1.61	1.39	1.31	0.88	0.72
Changes (%)	+33.33	+4.17	−3.30	−22.50	−25.00	−3.85	+3.64	+28.80	+13.01	+6.50	−13.73	−21.74

[a] See Table 1 for abbreviation definitions.

disappeared in the fungal-decayed wooden components, indicating that lignin was mainly demethylated, depolymerized, and degraded by fungal attack (Irbe et al. 2011), resulting in a reduction in its contents. By contrast, these absorption peak intensities, especially at 1,508, 1,460, and 1,424 cm^{-1} were higher than those in the nondecayed wood components seen in Figure 2, indicating a relative increase in lignin content. The increase in peak intensities after fungal attack might be related to the degradation of carbohydrates. However, the absorption peak at 1,260 cm^{-1}, which is attributed to guaiacyl-lignin, had disappeared and became two small absorption peaks at 1,270 and 1,232 cm^{-1}, which are attributed to syringyl-lignin. This finding reveals that guaiacyl-lignin was degraded by fungi, resulting in a decrease in guaiacyl units and an increase in syringyl units. A new absorption peak of 1,120 cm^{-1} was found, indicating an increase in lignin content.

Based on the analysis of absorption peak intensities, we concluded that the cellulose, hemicellulose, and lignin of Schima wood components were attacked by white-rot fungi. This finding is consistent with the microstructures of polarized light and fluorescence (Yang et al. 2020b). White-rot fungi degrade carbohydrates and lignin. Hence, we speculated that the Schima wood components were attacked by white-rot fungi.

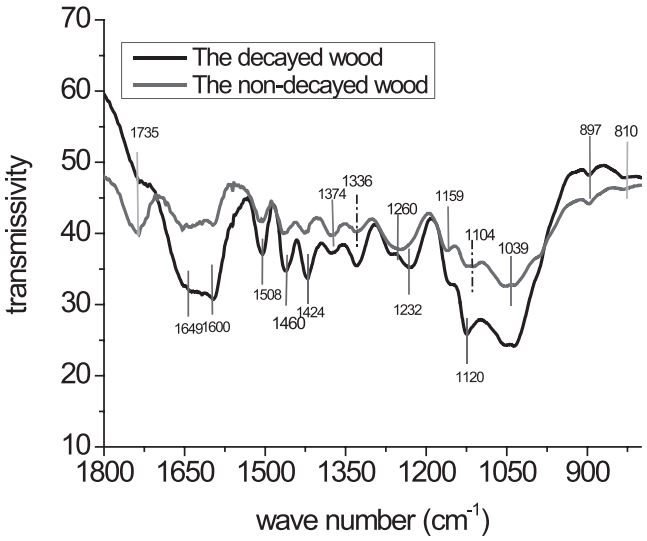

Figure 2.—Infrared spectrum of the Schima wood components: the region from 1,800 to 800 cm^{-1}.

Carbohydrate contents decreased as indicated by the values of H1159/H1508 and H1039/H1508, whereas the lignin contents increased as indicated by the values of H1508/H1159, H1508/H1039, H1649/H1039, and H1600/H1039 (Table 3). The reduction in carbohydrate contents indicated that the hemicellulose and cellulose of Schima wood components were more vulnerable to fungal decay. Table 3 also showed that the values of H1508/H1735 and H1508/H1374 decreased from 1.04 to 0.78 and from 1.04 to 1.00, respectively, with 25.00 and 3.83 percent reductions, respectively. This decrease might have been caused by serious lignin degradation resulting from fungal decay. Meanwhile, H1735/H1508 and H1374/H1508 increased from 0.96 to 1.28 and from 0.96 to 1.00, respectively, with associated increases of 33.33 and 4.18 percent, respectively (Table 3). These changes occurred because hemicellulose and cellulose were better able to resist fungal attack relative to lignin. This finding was in agreement with reports by Pandey and Pitman (2003) and Xu et al. (2013).

The H1374/H2900 ratio, representing the cellulose crystallinity index, decreased from 1.02 in the nondecayed wood components to 0.88 in the fungal-decayed wood components. Meanwhile, H1429/H897 decreased from 0.92 to 0.72 (Table 3). The associated reductions were 13.73 and 21.74 percent for H1374/H2900 and H1429/H897, respectively (Table 3). These results showed a decrease in crystallinity and were in good agreement with those of a previous study (Monrroy et al. 2011) and those obtained for red oak wood components discussed in this article.

Conclusions

The changes in chemical composition of red oak and Schima woods in the ancient building of Xichuan Guild Hall were analyzed with FTIR spectra, and the conclusions are as follows:

(1) The absorption peak intensities, chemical composition changes, and crystallinity index, which represent the structural contribution of carbohydrates in the red oak wood components, decreased by 55.70 percent in H1039/H1508, and 26.85 percent in H1370/H2900. These findings indicated that the brown-rot fungi had stronger preference to degrade hemicellulose and cellulose relative to lignin in the red oak wood components.

(2) The absorption peak intensities, chemical composition changes, and crystallinity index (which represented the structural contribution of carbohydrates in the Schima

wood components) decreased by 22.50 percent in H1039/H1508, and 21.74 percent in H1429/H897. Part of the structural contribution of lignin was also decreased by 25.00 percent in H1508/H1735 after decay. These findings indicated that not only cellulose and hemicellulose but also lignin in the Schima wooden components were attacked by white-rot fungi.

Acknowledgments

The authors gratefully acknowledge financial support from the Natural National Science Foundation of China (31700481), the Cross-Science Research Project of Nanyang Institute of Technology (230068), and Scientific Research Start-up Projects of Nanyang Institute of Technology (510144), Humanities and Social Sciences Research Project of Henan Province (2021-ZZJH-252).

Literature Cited

Arias, M. E., J. Rodríguez, M. I. Pérez, M. Hernández, O. Polvillo, J. A. González-Pérez, and F. J. González-Vila. 2010. Analysis of chemical changes in Picea abies wood decayed by different Streptomyces strains showing evidence for biopulping procedures. *Wood Sci. Technol*. 44(2):179–188.

Bari, E., M. G. Daryaei, M. Karim, M. Bahmani, O. Schmid, S. Woodward, M. A. Tajick-Ghanbary, and A. Sistani. 2019. Decay of Carpinus betulus wood by Trametes versicolor—An anatomical and chemical study. *Int. Biodeterior. Biodegrad*. 137:68–77.

Brischke, C., S. Stricker, L. Meyer-Veltrup, and L. Emmerich. 2019. Changes in sorption and electrical properties of wood caused by fungal decay. *Holzforschung* 73(5):445–455.

Chang, L., B. Rong, G. Xu, Q. Meng, and L. Wang. 2019. Mechanical properties, components and decay resistance of *Populus davidiana* bioincised by *Coriolus versicolor*. *J. Forestry Res*. 31:2023–2029. DOI:10.1007/s11676-019-00972-3

Choi, J. W., D. H. Choi, S. H. Ahn, S. S. Lee, M. K. Kim, D. Meier, O. Faix, and G. M. Scott. 2006. Characterization of trembling aspen wood (*Populus tremuloides* L.) degraded with the white rot fungus *Ceriporiopsis subvermispora* and MWLs isolated thereof. *Holz Roh-Werkst*. 64(5):415–422.

Croitoru, C., C. Spirchez, A. Lunguleasa, D. Cristea, I. C. Roata, M. A. Pop, T. Bedo, E. M. Stanciu, and A. Pascu. 2018. Surface properties of thermally treated composite wood panels. *Appl. Surf. Sci*. 438:114–126.

Fahey, L. M., M. K. Nieuwoudt, and P. J. Harris. 2019. Predicting the cell-wall compositions of solid *Pinus radiata* (radiata pine) wood using NIR and ATR FTIR spectroscopies. *Cellulose* 26(13–14):7695–7716.

Ferraz, A. and N. Durán. 1995. Lignin degradation during softwood decaying by the ascomycete Chrysonilia sitophila. *Biodegradation* 6(4):265–274.

Gao, S., L. H. Wang, and X. Q. Yue. 2019. Effect of the degree of decay on the electrical resistance of wood degraded by brown-rot fungi. *Can. J. Forest Res*. 49:145–153.

Guo, M. L., H. F. Lan, and J. Qiu. 2010. Wood Deterioration and Preservation. China Metrology Publishing House, Beijing. pp 163–168.

Huang, X. A., D. Kocaefe, Y. Kocaefe, Y. Boluk, and A. Pichette. 2012. Study of the degradation behavior of heat-treated jack pine (*Pinus banksiana*) under artificial sunlight irradiation. *Polym. Degrad. Stabil*. 97(7):1197–1214.

Ibrahim, M. N. M., N. N. M. Yusof, and A. Hashim. 2007. Comparison studies on soda lignin and soda anthraquinone lignin. *Malays. J. Anal. Sci*. 11(1):206–212.

Irbe, I., I. Andersone, B. Andersons, G. Noldt, T. Dizhbite, N. Kurnosova, M. Nuopponen, and D. Stewart. 2011. Characterization of the initial degradation stage of Scots pine (*Pinus sylvestris* L.) sapwood after attack by brown-rot fungus Coniophora puteana. *Biodegradation* 22(4):719–728.

Koyani, R. D. and K. S. Rajput. 2014. Light microscopic analysis of Tectona grandis L.f. wood inoculated with Irpex lacteus and Phanerochaete chrysosporium. *Eur. J. Wood Wood Prod*. 72(2):157–164.

Li, G. Y., A. M. Huang, T. F. Qin, and L. H. Huang. 2010. FTIR studies of Masson pine wood decayed by brown-rot fungi. *Spectrosc. Spect. Anal*. 30(8):2133–2136.

Li, S., Y. Gao, M. Brunetti, N. Macchioni, M. Nocetti, and S. Palanti. 2019. Mechanical and physical properties of Cunninghamia lanceolata wood decayed by brown rot. *Forest* 12:317–322.

Liu, C. W., M. L. Su, X. W. Zhou, R. J. Zhao, J. X. Lu, and Y. R. Wang. 2017. Analysis of content and distribution of lignin in cell wall of transgenic poplar with Fourier Infrared Spectrun (FTIR) and Confocal Laser Scanning Microscopy (CLSM). *Spectrosc. Spect. Anal*. 37(11):3404–3408.

Monrroy, M., I. Ortega, and M. Ramirez. 2011. Structural change in wood by brown rot fungi and effect on enzymatic hydrolysis. *Enzyme Microb. Technol*. 49(5):472–477.

Pandey, K. K. and H. C. Nagveni. 2007. Rapid characterization of brown and white rot degraded chir pine and rubber wood by FTIR spectroscopy. *Eur. J. Wood Wood Prod*. 65(6):477–481.

Pandey, K. K. and A. J. Pitman. 2003. FTIR studies of the changes in wood chemistry following decay by brown-rot and white-rot fungi. *Int. Biodeterior. Biodegrad*. 52(3):151–160.

Solár, R., S. Kurjatko, M. Mamon, B. Košiková, E. Neuschlová, E. Výbohová, and J. Hudec. 2007. Selected properties of beech wood degraded by brown-rot fungus Coniophora puteana. *Drv. Ind*. 58(1):3–11.

Stark, N. M. and L. M. Matuana. 2004. Surface chemistry changes of weathered HDPE/wood-flour composites studied by XPS and FTIR spectroscopy. *Polym. Degrad. Stabil*. 86(1):1–9.

Stark, N. M. and L. M. Matuana. 2007. Characterization of weathered wood-plastic composite surfaces using FTIR spectroscopy, contact angle, and XPS. *Polym. Degrad. Stabil*. 92(10):1883–1890.

Sun, H., Y. Yang, Y. X. Han, M. J. Tian, B. Li, L. Han, A. F. Wang, W. Wang, R. Zhao, and Y. M. He. 2020. X-ray photoelectron spectroscopy analysis of wood degradation in old architecture. *BioResources* 15(3):6332–6343.

Tamburini, D., J. J. Lucejko, B. Pizzo, M. Y. Mohammed, and R. Sloggett. 2017. A critical evaluation of the degradation state of dry archaeological wood from Egypt by SEM, ATR-FTIR, wet chemical analysis and Py(HMDS)-GC-MS. *Polym. Degrad. Stabil*. 146:140–154.

Tomak, E. D., E. Topaloglu, E. Gumuskaya, U. C. Yildiz, and N. Ay. 2013. An FTIR study of the changes in chemical composition of bamboo degraded by brown-rot fungi. *Int. Biodeterior. Biodegrad*. 85:131–138.

Wentzel, M., A. Rolleri, H. Pesenti, and H. Militz. 2019. Chemical analysis and cellulose crystallinity of thermally modified Eucalyptus nitens wood from open and closed reactor systems using FTIR and X-ray crystallography. *Eur. J. Wood Wood Prod*. 77(4):517–525.

Xu, G. Q., L. H. Wang, J. L. Liu, and J. Z. Wu. 2013. FTIR and XPS analysis of the changes in bamboo chemical structure decayed by white-rot and brown-rot fungi. *Appl. Surf. Sci*. 280:799–805.

Yang, Y., J. X. Lu, and B. Li. 2020a. The Mathematical Model of Heat and Mass Transfer in Alder Birch Wood and the Color Control during the Thermo-Vacuum Treatment. Chemical Industry Press, Bingjing. 108 pp.

Yang, Y., H. Sun, B. Li, L. Han, A. F. Wang, W. Wang, Y. M. He, and R. Zhao. 2020b. Study on the identification and the extent of decay of the wooden components in the Xichuan Guild Hall ancient architectures. *Int. J. Archit. Herit*. DOI:10.1080/15583058.2020.1786190

Yang, Y., T. Y. Zhan, J. X. Lu, and J. H. Jiang. 2015. Influences of thermo-vacuum treatment on colors and chemical compositions of alder birch wood. *BioResources* 10(4):7936–7945.

Zeng, Y. L., X. W. Yang, H. B. Yu, X. Y. Zhang, and F. Ma. 2012. The delignification effects of white-rot fungal pretreatment on thermal characteristics of moso bamboo. *Bioresour. Technol*. 114:437–442.